Multidisciplinary Design Optimization for a Blended Wing Body Transport Aircraft with Distributed Propulsion

Leifur Thor Leifsson, Andy Ko, William H. Mason,
Joseph A. Schetz, Raphael T. Haftka, and Bernard Grossman

MAD Center Report 2005-05-01

Supported by the System Analysis Branch at NASA Langley
Under Grant NAG-1-02024

Multidisciplinary Analysis and Design Center
for Advanced Vehicles

Virginia Polytechnic Institute & State University
Blacksburg, VA 24061-0203

Contents

List of Figures

List of Tables

Multidisciplinary Design Optimization for a Blended Wing Body Transport Aircraft with Distributed Propulsion

Leifur T. Leifsson*, Andy Ko, William H. Mason, Joseph A. Schetz,

Bernard Grossman, and Raphael T. Haftka

Multidisciplinary Analysis and Design (MAD) Center for Advanced Vehicles

Virginia Polytechnic Institute and State University

Blacksburg, VA 24061-0203

Abstract

A distributed propulsion concept for aircraft is considered. The concept involves replacing a small number of large engines with a moderate number of small engines and ducting part of the engine exhaust to exit out along the trailing edge of the wing. Models to describe the effects of this distributed propulsion concept were formulated and integrated into an MDO formulation. The most important effect modeled is the impact on the propulsive efficiency when there is blowing out of the trailing edge of a wing. An increase in propulsive efficiency is attainable with this arrangement as the trailing edge jet 'fills in' the wake behind the body, improving the overall aero-

*Corresponding author. Department of Aerospace and Ocean Engineering, 215 Randolph Hall, Virginia Polytechnic Institute and State University, Blacksburg, VA 24061-0203. Phone: 1-540-8715296, Fax: 1-540-2319632, e-mail: leifur@vt.edu

dynamic/propulsion system, resulting in an increased propulsive efficiency. Other models formulated include the effect of the trailing edge jet on the induced drag, longitudinal control through thrust vectoring of the trailing edge jet, increased weight due to the ducts, and thrust losses within the ducts. The Blended Wing Body (BWB) aircraft was used as a testbed to study the distributed propulsion concept. Two different BWB configurations were optimized. A conventional propulsion BWB with four pylon mounted engines and a distributed propulsion BWB with eight boundary layer ingestion inlet engines. The results show that significant weight penalty is associated with the distributed propulsion system that realistically cannot be overcome by the potential savings by effects on the induced drag, elimination of trailing edge flaps, and by 'filling in' the wake. However, other potential benefits of distributed propulsion need to be considered when evaluating the overall performance and characteristics of the design, such as improved safety due to engine redundancy, less critical engine-out condition, gust load/flutter alleviation, increased affordability due to smaller, easily-interchangeable engines.

Keywords: distributed propulsion, propulsive efficiency, jet wing, jet flap, multidisciplinary design optimization, blended-wing-body

Nomenclature

AR	Aspect ratio
c	Chord length
C_D	Drag coefficient
C_{Di}	Induced drag coefficient
$C_{Di_{DP}}$	Distributed propulsion induced drag coefficient
C_{D_p}	Profile drag coefficient
C_{D_w}	Wave drag coefficient
C_J	Jet momentum flux coefficient
	$= \frac{J}{\frac{1}{2}\rho U_\infty^2 S_{ref}}$
C_L	Lift coefficient
J	Jet thrust
L/D	Lift to drag ratio
M	Mach number
S_{ref}	Wing planform reference area
sfc	Specific fuel consumption
t	Air temperature at a given altitude
T	Total thrust from engine
	$= T_{bleed} + T_{excess}$
T_{bleed}	Bleed part of thrust from engine
T_{excess}	Excess part of thrust from engine

T_{jet}	Jet thrust
	$= \eta_d T_{bleed}$
T_{net}	Bleed part of thrust from engine
	$= T_{jet} + T_{excess}$
T_0	Maximum sea level static thrust
$TOGW$	Takeoff gross weight
U_∞	Free stream velocity
V_{min}	Minimum velocity at approach
w_d	Duct weight factor
α	Angle of attack
η_d	Duct efficiency
η_{DP}	Distributed propulsion factor
η_P	Froude propulsive efficiency
η_T	Engine internal thermal efficiency
κ_l	sfc factor
Λ	Wing quarter chord sweep angle
ρ	Density of air
Θ	Ratio of jet thrust to net thrust
	$= \frac{T_{jet}}{T_{net}} \equiv \frac{C_{D_p}+C_{D_w}}{C_D}$

1 Introduction

Multidisciplinary Design Optimization (MDO) has been receiving increased interest in the aerospace industry as a valuable tool in aircraft design [1, 2, 3]. The use of MDO in conceptual and preliminary design of innovative aircraft concepts is but one application where it provides the designer with better insight into the coupled nature of different aerospace disciplines related to aircraft design. In a general MDO aircraft design framework, different analysis modules or their surrogates representing the different disciplines, such as structures and aerodynamics, are coupled with an optimizer to find an optimum design subject to specified design constraints. This provides a means of designing planes requiring tightly coupled technologies. This paper describes the use of an MDO framework to design a distributed propulsion Blended-Wing-Body (BWB) aircraft [4]. The BWB is a unique tailless aircraft. The high level of integration between the wing, "fuselage", engines, and control surfaces inherent in the BWB design allows it to take advantage of the synergistic nature between the different aircraft design disciplines resulting in an aircraft with better performance than a conventional design. Figure 1 shows a BWB concept with conventional propulsion (few larger pylon mounted engines). With the distributed propulsion concept integrated into the BWB aircraft design, MDO will be used to identify the advantages of this aerodynamics-propulsion integration and highlight its benefits.

2 The Distributed Propulsion Concept

The idea of using distributed propulsion has been suggested with the objective of reducing noise [5]. Distributing the propulsion system using a number of small engines instead of a few large ones could reduce the total propulsion system noise. There are other potential benefits of distributed propulsion. One advantage is its improved safety due to engine redundancy. With numerous engines, an engine-out condition is not as critical to the aircraft's performance in terms of loss of available thrust and controllability. The load redistribution provided by the engines has the potential to alleviate gust load/flutter problems, while providing passive load alleviation resulting in a lower wing weight. There is also the possible improvement in affordability due to the use of smaller, easily-interchangeable engines.

One suggested distributed propulsion arrangement is to place an array of small engines distributed along the wings and/or around the fuselage under cowls as depicted schematically in Figure 2. We find this arrangement to be unattractive. The reason is the basic conflict between the axisymmetric geometry of jet or propeller engines and the planar space under the cowl. If the engines are turbojets, little additional air will be entrained to flow under the cowl resulting in poor system propulsive efficiency. If the engines are turbofans, the flow in the irregular spaces under the cowl and surrounding the fans will have high drag and will not contribute to propulsion. Thus, we have rejected further consideration of this arrangement. Rather, we have selected a concept that ducts part of

the exhaust from a moderate number of wing mounted engines out of the trailing edge across part or all of the span of the wing. Such a concept could be employed as a seamless high-lift system, dispensing with conventional high-lift systems that are major sources of noise. Figure 3 shows a planform view of a BWB with distributed propulsion configuration as suggested here and Figure 4 shows two wing cross sections of this concept. Exhausting out the trailing edge of the wing is similar to jet wing and jet flap concepts.

The jet wing concept can be described as an arrangement on a wing where a thin sheet of air from the engine is ejected out of a slot near or at the trailing edge. This utilizes the available power of the engine for thrust and lift augmentation. The jet flap is an arrangement that ejects a thin sheet of high velocity air with a downward inclination out of a slot near or at the trailing edge to obtain high lift. Its application is associated with the generation of powered or high lift capabilities. While both concepts are similar in the sense that air from the engine is ejected out of the trailing edge of the wing. The difference lies in their application. The jet flap concept involves a large downward deflection of the jet sheet at an angle with respect to the free stream, usually in the context of STOL (Short takeoff and landing) aircraft configurations. The jet wing concept does not usually employ a deflection in the angle of the jet sheet. Two experimental aircraft demonstrated these concepts in flight [6, 7].

The distributed propulsion concept investigated here is a hybrid of the jet wing, jet flap and conventional propulsion concepts. While the jet exhausted out of the trailing edge will not be deflected at high angles during large portions of the aircraft's mission (jet wing

concept), it will be deflected at a modest angle to replace conventional flap systems and elevons (jet flap concept). Unlike both the jet wing and jet flap concept, the distributed propulsion concept only ducts part of the engine exhaust out of the trailing edge, with the remaining exhaust using conventional nozzles.

3 Distributed Propulsion Models

3.1 Propulsive Efficiency

Kuchemann suggested in 1938 [8]* that an improvement in propulsive efficiency could be achieved with the jet wing concept. Propulsive efficiency is improved because the jet exiting the trailing edge of the wing 'fills in' the wake behind the wing. This approach is commonly implemented in ships and submarines, having a streamlined axisymmetric body (neglecting the sail and the control surfaces) and a single propeller on the axis. Although the wake is not perfectly filled, this arrangement tends to maximize the propulsive efficiency of the entire system [9]. It is expected that a similar improvement in propulsive efficiency can be achieved with a distributed propulsion configuration that ducts some of the engine exhaust out of the trailing edge of the aircraft. A mathematical assessment

*The original reference to Kuchemann has been cited to be in: "On the Possibility of Connecting the Production of Lift with that of Propulsion", M.A.P. Volkenrode, Reports and Translations No. 941 - Nov., 1947, APPENDIX I, Kuchemann, D., "The Jet Wing". However, we were unable to obtain a copy of this reference.

of this hypothesis can be found in [10, 11].

To illustrate our approach to distributed propulsion we consider a two-dimensional, non-lifting, self-propelled vehicle with an engine as shown in Figure 5. The wake of the body is taken as independent of the jet from the engine. For the system to be self-propelled, the drag associated with the velocity deficit due to the wake is balanced by the thrust of the engine. The loss in propulsive efficiency is due to any net kinetic energy left in the wake (characterized by the non-uniformities in the velocity profiles) compared to that of a uniform velocity profile. For this case, a typical Froude Propulsion Efficiency for a high bypass ratio turbofan at Mach 0.85 is 80% [12].

Now, consider a distributed-propulsion configuration where the jet and the wake of the body are combined, as shown in Figure 6. In an ideal distributed-propulsion system, the jet will perfectly 'fill in' the wake creating a uniform velocity profile. The kinetic energy added to the flow by the propulsor compared to that of a uniform velocity profile is therefore zero, which results in a Froude Propulsive Efficiency of 100%. In practice, the jet does not exactly 'fill in' the wake but produces smaller non-uniformities in the velocity profile as illustrated in Figure 7. However, this velocity profile will result in a smaller net kinetic energy than that of the case shown in Figure 4, where the body and engine are independent. The efficiency associated with a distributed propulsion configuration will be bounded by the efficiency of the decoupled body/engine case (nominally at 80%) and the perfect distributed propulsion configuration of 100%. It should be noted, however, that we have not included the effect the jet has on the pressure distribution of the body.

We expect that the jet will entrain the flow over the surface and increase the drag, but this effect is not modeled here.

Now consider a lifting body with an engine in a distributed propulsion configuration. In this case, the drag on the system is not only due to the viscous drag but also the drag due to the downwash. This means that the engine jet now 'overfills' the wake. Therefore, even in a perfect system, a 100% Froude Propulsive Efficiency is not attainable. In the perfect system of this configuration, part of the jet would be used to perfectly 'fill in' the wake while the remaining jet would be in the free stream away from the body and used to overcome the induced drag. This arrangement is like that of our distributed propulsion concept illustrated in Figures 3 and 4. If the induced drag constitutes about 50% of the total drag (viscous drag + induced drag), as in well designed wings, then the maximum possible increase in Froude Propulsive Efficiency will be half of that in the non-lifting body case, i.e. the Froude Propulsive Efficiency using a nominal high bypass ratio turbofan in a distributed-propulsion setting would be between 80% -90%.

From the above example for a subsonic lifting body, we see that the upper limit of the Froude propulsive efficiency is determined by the ratio of the viscous drag to the total drag. In the same way, for a lifting body in transonic flow, the upper limit of the Froude propulsive efficiency is determined by the ratio of the viscous and wave drag to the total drag. The wave drag is included because the presence of shocks on the body affects the size and shape of the wake behind the wing/body.

In an aircraft design performance assessment, the Froude Propulsive Efficiency can be

reflected in the performance in terms of the thrust specific fuel consumption (sfc). We should expect that an increase in the Froude Propulsive Efficiency will result in a reduction in sfc, improving the aircraft's overall performance.

To relate the Froude Propulsive Efficiency to sfc, consider the approximate relation given by Stinton [13]

$$sfc = \frac{U_\infty}{\kappa_l \eta_P \eta_T}, \tag{1}$$

where U_∞ is the freestream velocity, κ_l is the SFC factor (determined to be 4000 ft-hr/s by Stinton [13]), η_P is the Froude propulsive efficiency, and η_T is the engine internal thermal efficiency. Assuming a constant free stream velocity, sfc factor and internal engine thermal efficiency, we can obtain the following relation

$$\frac{sfc_1}{sfc_2} = \frac{\eta_{P_1}}{\eta_{P_2}}. \tag{2}$$

Hence, given a baseline propulsive efficiency and sfc, a new sfc can be calculated for an increase in propulsive efficiency. With the maximum and minimum limits in attainable propulsive efficiency determined, we would expect that only a percentage of this possible increase in propulsive efficiency could be achieved.

3.2 Induced Drag

A key theory in describing and analyzing the jet wing is Spence's theory [14, 15, 16]. Spence extended thin airfoil theory to describe airfoil and wing performance with a jet wing in terms of the jet coefficient C_J, which is defined as

$$C_J = \frac{J}{\frac{1}{2}\rho U_\infty^2 S_{ref}}, \tag{3}$$

where J is the jet thrust, ρ is density, and S_{ref} is the wing planform reference area. Using Spence's Theory, the induced drag of an aircraft under an elliptical load distribution can be described as

$$C_{Di_{DP}} = \frac{C_L^2}{\pi AR + 2C_J}, \tag{4}$$

where C_L is the lift coefficient and AR is the wing aspect ratio. Comparing Equation (4) with the induced drag coefficient equation for a non-jet-winged wing with an elliptical load distribution, we find the addition of the factor $2C_J$ in the denominator that describes the influence of the jet wing on the induced drag of the wing. To implement the effects of the jet on the induced drag of the wing, the induced drag is calculated for the equivalent wing with out the jet, and then corrected with the following ratio

$$\frac{C_{Di_{DP}}}{C_{Di}} = \frac{1}{1 + \frac{2C_J}{\pi AR}}. \tag{5}$$

A typical value of the jet coefficient is about 0.03. Therefore, it is clear that the effect of the jet on the induced drag is negligible.

3.3 Control/Propulsion Integration

In the distributed propulsion BWB configuration, the elevon controls are replaced with a vectored jet wing control system. This system controls the BWB longitudinally by changing the deflection angle of the jet exiting the trailing edge of the wing.

To estimate the effects of the jet deflection angle on the lift and pitching moment of the aircraft, Spence's theory [14] is used. Spence's two dimensional theory extends the methods of thin-airfoil theory to give a solution for the inviscid incompressible flow past a thin airfoil at a small angle of attack (α), when a thin jet exits the trailing edge at a small deflection angle (τ). The method provides an estimate of the lift and pitching moment coefficient of the airfoil in terms of the jet coefficient, C_J. This theory was extended to a three-dimensional wing, corrected to account for wing sweep, to estimate the effects of the jet wing on the lift and pitching moment coefficients. This formulation compared well with a vortex lattice method for various wing planforms at $C_J = 0$. For $C_J > 0$, the formulation produced expected differences with a vortex lattice method (that corresponds to a wing at $C_J = 0$). Details of the formulation and the verification of the results can be found in [11].

3.4 Duct Modeling

There will be duct weight and thrust losses associated with ducting some of the engine exhaust through the trailing edges of the aircraft.

The duct weight is simulated by a duct weight factor applied to the propulsion system weight. There is a possibility that the duct weight does not scale linearly with the propulsion system weight. It has been suggested that perhaps the duct weight scales more closely with the jet velocity or the mass flow rate of the engine. However, the distributed propulsion BWB MDO framework scales the duct weight through the use of a factor applied to the propulsion system weight. A nominal factor of 10-20% has been deemed realistic.

To simulate the duct losses on the portion of the thrust that is exhausted out of the trailing edge, a duct efficiency factor is applied to the that portion of the aircraft thrust. Let the total thrust produced by a turbofan engine be

$$T = T_{bleed} + T_{excess}. \tag{6}$$

The bleed part is diverted through the duct and out the trailing edge and the excess part goes out the rear of the engine, see figure 14. Then the net thrust available from the propulsion system is

$$T_{net} = T_{jet} + T_{excess}, \tag{7}$$

where $T_{jet} = \eta_d T_{bleed}$ and η_d is the duct efficiency. The amount exhausted out the trailing edge should be enough to 'fill in' the wake behind the aircraft. In the present formulation this amount has been determined to be equal to the profile and wave drag of the wing. So, the ratio of jet thrust to net thrust is set to the ratio of profile and wave drag to total drag of the vehicle, or

$$\frac{T_{jet}}{T_{net}} = \Theta, \tag{8}$$

where

$$\Theta \equiv \frac{C_{D_p} + C_{D_w}}{C_D}. \tag{9}$$

Now the ratio of net thrust and total thrust can be determined as

$$\frac{T_{net}}{T} = \left(1 + \frac{1 - \eta_d}{\eta_d}\Theta\right)^{-1}. \tag{10}$$

Initially, the effect of the duct efficiency was introduced through equation (10) in the BWB MDO formulation. This led to results that were not quite what was expected. With this formulation the optimizer was able to increase the total thrust T of the engine to overcome any thrust loss due to the ducts and still satisfy the critical design constraints,

which is the second segment climb gradient constraint in this case. By increasing the thrust the engines will get larger and heavier. Then two things will drive the design. First, because the engines are heavier there is increased load alleviation on the wing. This gives incentive to increase the span and aspect ratio and thereby increasing the lift-to-drag ratio, which in turn will allow for a decrease in required fuel weight. Second, since the engines are larger the specific fuel consumption (sfc) will decrease, which also will allow a decrease in fuel weight. So, by decreasing the duct efficiency the new aircraft design will be more efficient, that is, it will require less fuel to finish the mission, which of course is not realistic. This formulation has no adverse effects, except for increased propulsion system weight, of having thrust loss due to the ducts.

Instead of accounting for the duct efficiency as a direct loss in thrust, it is more appropriate to account for the effect on the engine workload. The drag of the vehicle is constant for a given design at given conditions. Therefore, the thrust loss should be overcome by increased thrust from the given engines, but not by increasing the size of the engine. Increased workload on the engines means increased fuel flow. So, the effect of thrust loss should be accounted for by increasing the sfc of the engines.

The specific fuel consumption for an engine is defined to be

$$sfc = \frac{\dot{w}_f}{T}, \tag{11}$$

where $\dot{w}_f$ is the fuel flow rate. By using equations (10) and (12 a relation between the

new sfc_{net}, which accounts for the thrust loss, and the old sfc can be obtained as

$$sfc_{net} = \left(1 + \frac{1 - \eta_d}{\eta_d}\Theta\right) sfc. \tag{12}$$

If the duct efficiency is 95% and the ratio of profile and wave drag to total drag is 0.5, then the increase in sfc is approximately 2.6%. So, with this formulation, the optimizer will see an increase in sfc by 2.6%, but not a loss in total thrust by 2.6%.

4 BWB MDO Framework

4.1 MDO Formulation

A total of 23 design variables are used in the MDO setup, given in Table 1, and they include aircraft geometric properties, described in the next section, and operating parameters such as altitude, sea level static thrust and fuel weight. The design constraints are 27, given in Table 2, and they cover the aircraft geometry, takeoff, climb, cruise, and landing. The most important design parameters are listed in Table 3, and they are related to the aircraft mission, distributed propulsion, and high lift systems. The objective function is to minimize $TOGW$. ModelCenter is used to integrate different analysis models and setup the MDO framework.

4.2 BWB Geometric Description

The BWB planform is described using a parametric model with a relatively small number of design parameters. Five spanwise stations are used to define the shape of the planform, see Figure 8. The geometric properties at those stations are design variables. They are chord length, airfoil thickness, and quarter-chord sweep. A straight line wrap method is used to define the properties of the aircraft between the span stations.

The center inboard section of the BWB is double decked. The passengers are on the upper deck, between the forward and rear spar, and are seated in a three-class configuration in six aisles. To ensure that there is enough cabin space for the number of passengers carried on the BWB, an average of 8.5 ft^2 of cabin floor area per passenger is assigned [17]. The cargo is stored on the lower deck, forward of the rear spar. Behind the rear spar is the afterbody that houses the aircraft systems and emergency exit tunnels.

The definition of height and length of the double deck center section is shown is Figure 9. The height is assumed to be 90% of the maximum thickness of the airfoil section and the length is the distance between the forward and rear spars. Thickness constraints are used to ensure that the airfoil is thick enough at the forward and rear spars to enclose the double deck section. This is done by using a generic airfoil shape to define the thickness at the spar locations.

The fuel tanks are located in the wing sections outboard of the passenger cabin. They extend to the 95% semi-span location of the wing. Slats are located at the leading edge of

the wing, outboard of the cabin section. Trailing edge flaps are located inboard of the last wing section, where the ailerons are located. The distributed propulsion configuration does not include the trailing edge flaps. Instead the trailing edge jet is deflected for high lift generation.

4.3 Aerodynamics

The aerodynamics module models the induced, wave, friction, and trim drag of the aircraft. This module evolved from our previous work on truss-braced wing concepts [18].

The induced drag is determined from a Trefftz plane analysis for minimum induced drag [19]. The model also calculates the load distribution on the wing and allows for non-planar surfaces, which provides the capability to model winglets on the BWB.

The wave drag calculation uses the Korn equation [20] to estimate the transonic wave drag of a wing. Simple sweep theory is used to account for sweep. The wing geometry is divided into a number of spanwise strips and the wave drag model estimates the drag as a function of an airfoil technology factor, thickness to chord ratio, section lift coefficient and sweep angle for each individual strip.

The friction drag model is based on applying form factors to an equivalent flat plate skin friction drag analysis. The amount of laminar flow on the BWB is estimated by interpolating results from the Reynolds number vs. sweep data obtained from the F-14

Variable Sweep Transition Flight Experiment [21] and wind tunnel test data from Boltz et al. [22]. This model is applied to the aircraft wing, winglets, and engine nacelles.

Trim drag at cruise is calculated as the difference between the minimum induced drag and induced drag at the estimated aircraft cruise cg location. The induced drag analysis is determined using a Trefftz plane analysis [23].

4.4 Propulsion System Analysis

The propulsion system analysis model calculates the weight, thrust and sfc performance of the engines as a function of flight Mach, altitude, max sea level static thrust, and sea level static sfc. The size and weight of the nacelles and pylons are also calculated.

An engine weight model was constructed that scales the engine weight with the max sea level static thrust. The resulting model is

$$W_{eng} = 18.4822 T_0^{0.6} - 2500, \tag{13}$$

where T_0 is the max sea level static thrust. This engine weight model was not obtained by using statistical analysis of available engine data. It was constructed to represent a quantitative difference between smaller and larger engines, which is that fewer larger engines will weigh less than more smaller engines for the same overall thrust of the propulsion system. A plot of the engine weight model and data for gas turbine engines (turbojets and turbofans) is shown in Figure 10. The weight of the nacelle and the

pylon are a function of the engine weight and are calculated using equations provided by Liebeck et al. [17].

Rubber sizing models were also constructed for the nacelle diameter and length by using a representative engine, GE-90-like, and available data for engine max envelope diameter and length as a function of max sea level static thrust. The nacelle diameter model is

$$D_{nac} = 0.4367 T_0^{0.5}, \tag{14}$$

and the nacelle length model is

$$L_{nac} = 2.8579 T_0^{0.4}. \tag{15}$$

Figures 11 and 12 show these nacelle size models plotted with data for maximum envelope diameters of gas turbine engines.

GE-90-like engine deck models are used to describe the changes in thrust and sfc with altitude and airspeed. The models were found by regression analysis of engine data are due to Gundlach [24]. The thrust model is

$$\frac{T}{T_0} = \left(0.6069 + 0.5344\left(0.9001 - M\right)^{2.7981}\right)\left(\frac{\rho}{\rho_{sl}}\right)^{0.8852} \tag{16}$$

where T is engine thrust at given altitude and Mach, T_0 is the max sea level static thrust, M is the Mach number, ρ is the air density at the given altitude, and ρ_{sl} is air density

at sea level. The sfc model is [24]

$$sfc = \left(\frac{t}{t_{sl}}\right)^{0.4704} (sfc_{sls} + 0.4021M)\,. \tag{17}$$

where t is the air temperature at the given altitude, t_{sl} is the temperature at sea level, and sfc_{sls} is the sea level static specific fuel consumption. In our previous study CITE it was assumed that sfc_{sls} is independent of engine size. However, it is clear that as the engine gets smaller in size the performance will be degraded and sfc_{sls} will increase. To quantify this effect the Rolls-Royce engine family was chosen and the sfc at cruise power was plotted versus the maximum sea level static thrust of the engine, see Figure 13. A second order polynomial was fitted to the data of sfc at cruise power. Assuming that the cruise condition is at Mach 0.85 and at an altitude of 35,000 ft the sea level static sfc is estimated using Gundlach's model. Now Gundlach's model gives the variation in SFC with altitude, airspeed and the sea level static sfc, which is now a function of maximum sea level static thrust. It is clear from this data that smaller engines will have higher sfc and this will have adverse effects on distributed propulsion.

The distributed propulsion arrangement adopted here for the BWB aircraft calls for some of the engine exhaust to be ducted out of the aircraft trailing edge. It also calls for a moderate number of engines (about 8) along the span. This arrangement might place the inlets in the path of the boundary layer developing on the body of the aircraft. It is possible to use traditional pylon mounted engines, but it is not clear how to duct part of

the exhaust from that type of engine mounting. Boundary layer ingesting (BLI) inlets require the engine to be embedded into the wing, which in turn makes it relatively easy to duct part of the engine exhaust out the TE of the wing. However, using BLI inlets will result in a performance reduction of the engines due to an adverse fan pressure recovery which will lead to an increase in SFC. Gorton et al. [25] have shown that active flow control can be used to enhance the performance of BLI inlets and overcome the increase in engine sfc. In this study we will assume that the sfc of BLI inlet engines will be the same as pylon mounted engines.

4.5 Weight Analysis

The wing bending material weight is calculated using a double plate model [26]. The remaining components of the wing weight are estimated using NASA Langley's Flight Optimization Software (FLOPS) [27]. This model takes into account the geometry of the individual wing sections, and the number and position of the engines on the wing for load alleviation.

The calculation of individual component weights, such as passenger cabin, afterbody, landing gear, furnishings and fixed weights, for the BWB is based on the analysis done by Liebeck et al. [17]. However, due to the unconventionality of the cabin and low-fidelity of the weight analysis, a 15,000 lb weight penalty is added. A further 10% increase in fixed weight was also added.

4.6 Aircraft Performance

The aircraft performance module calculates both aircraft cruise and field performance. For the cruise performance the aircraft range and top of climb rate of climb are calculated. Range is calculated based on the Breguet range equation.

For the field performance, the second segment climb gradient, balanced field length, landing distance, missed approach climb gradient and approach velocity are calculated. The balanced field length calculation is based on an empirical estimation by Torenbeek [28], while the landing distance is determined using methods suggested by Roskam and Lan [29].

4.7 Stability and Control

Only longitudinal control is considered in the MDO formulation. The analysis compares the longitudinal center of gravity (cg) location with the longitudinal control capability of the aircraft through elevons (conventional design) or the thrust vectoring system (distributed propulsion design) based on two assessment criteria. These criteria draw in part on those used by the European MOB project [30]. The two criteria are evaluated at the approach flight phase. Based on a minimum approach velocity of 140 knots, a minimum velocity, V_{min} of 110 knots is used for the longitudinal control evaluation. This is done to provide a 30% safety margin on approach. The two criteria that are used are:

- Maximum elevon deflection boundary at V_{min}

- Maximum angle-of attack boundary at V_{min}

The maximum elevon deflection boundary at V_{min} criteria requires that the cg location of the aircraft should be within limits such that the aircraft elevon trim angles do not exceed the maximum deflection angles of $\pm 20^o$. The angle of attack at this condition is that required to provide the required lift during 1g flight.

The maximum angle of attack boundary at V_{min} criteria requires that the aircraft cg is at a location such that the angle of attack of the elevon-trimmed aircraft does not exceed the stall angle of attack. Currently, the stall angle of attack is taken to be at 27^o.

These two criteria set forward and rear cg limits on the aircraft cg location at four critical weight conditions. Those conditions are at:

- Operational empty weight
- Operational empty weight + Full fuel weight
- Zero fuel weight
- Takeoff gross weight ($TOGW$)

These design conditions are enforced in the MDO framework using inequality constraints.

5 BWB Model Validation

The BWB model was validated by analyzing published Boeing BWB configurations. The latest Boeing designs have a mission of 7,750 nm at Mach 0.85 carrying 478 passengers [31]. However, currently the only data publicly available for those designs is a comparison of the BWB-450 with the Airbus A380 made by Liebeck [31] and is based on a mission of approximately 480 passengers and approximately 8,700 nm range. Based on available data for the A380, it is possible to calculate approximately the weight of the BWB-450. This data is the reference point in our validation of the BWB model.

The reference BWB-450-like planform is shown in Figure 15 along with some performance and weight results of an analysis. A break down of the weight analysis is shown in Table 4. Compared to our estimate of the BWB-450, the difference in $TOGW$ is less than 3%, which is acceptable. Furthermore, the difference in cruise L/D is less than 1.4%, based on results published by Roman et al. [32].

6 MDO Study: Effects of Distributed Propulsion

6.1 Description

Two different configurations of BWB designs are studied, a distributed propulsion BWB aircraft and a conventional propulsion BWB aircraft used as a comparator. An eight engine configuration with boundary layer ingestion inlets is used for the distributed propul-

sion BWB aircraft design while the conventional propulsion BWB aircraft has a pylon mounted four engine configuration. For the optimum distributed propulsion BWB design, the engines are evenly spaced inboard of the 70% semi-span location on the wing ($\eta_{eng} = 0.1, 0.3, 0.5, 0.7$). Part of the engine exhaust will exit through the trailing edge across the entire span of the aircraft. The ducts used to divert the engine exhaust out the trailing edge are assumed to have an efficiency of η_d. To account for the weight of the ducts, the weight of the propulsion system is increased by w_d. No detailed studies have yet been done to determine a nominal value for these parameters. However, duct efficiency of 95-97% and duct weight factor of 10-20% are judged to be realistic. Therefore, two optimized configurations were obtained. An 'optimistic' design with $\eta_d = 97\%$ and $w_d = 10\%$ and a 'conservative' design with $\eta_d = 95\%$ and $w_d = 20\%$.

To examine the individual distributed propulsion effects on the BWB design, six additional optimized BWB designs were obtained. These designs, described in Table 5, were created by adding each distributed propulsion effect individually to the conventional BWB configuration and obtaining an optimum solution. The first design is a conventional propulsion BWB with four pylon mounted engines. The second design has eight pylon mounted engines. In the third design, the pylon mounted engines are replaced with boundary layer ingestion inlet engines. This change is modelled by removing the pylon and considering only half the wetted area of the nacelles when calculating their profile drag. The first distributed propulsion effect is introduced in design number four. Here a part of the exhaust is ducted out the trailing edge, but only induced drag effects are

included. This design also includes the trailing edge flaps for wing weight calculation. The trailing edge flaps are removed in design number five. Design number six introduces the duct weight by increasing the propulsion system weight by 10-20%. Duct efficiency is reduced from 100% to 95-97% in design seven. The last design has the distributed propulsion factor which gives, if possible, approximately the same $TOGW$ as the first design. This is the break even point and any further savings by 'filling in' the wake will produce a distributed propulsion BWB that is more efficient than a conventional propulsion one.

6.2 Results

The results for both the conventional propulsion BWB and the distributed propulsion configuration along with each intermediate optimized designs are presented in Table 6. To analyze the results it is best to discuss each adjacent cases.

Cases 1 and 2: Designs in cases 1 and 2 represent a change in the number of engines, from four large engines to eight smaller engines. Design 1 has engines positioned at $\eta = 0.1$ and 0.3, whereas design 2 has the engines positioned at $\eta = 0.1$, 0.3, 0.5, and 0.7. As can be seen from Table 6, the span increases from 239.5 ft to 245.5 ft and the aspect ratio from 4.28 to 4.45, for cases 1 and 2 respectively. There are mainly two things driving this change. Firstly, by distributing the engines along the span, load alleviation on the wing is increased. This effect gives incentive to increase

the span and aspect ratio and thereby the lift-to-drag ratio is increased. In this case the lift-to-drag ratio has increased by 1.4%. Secondly, the thrust per engine is reduced and so the engines get smaller in size. As a result the sfc increases by 13.5% and the fuel weight increases by 16.5%. This effect also gives incentive to increase the span and aspect ratio to increase the cruise efficiency. The resulting design 2 has a $TOGW$ that is 65,935 lb (or 7.6%) heavier than design 1. However, the total thrust is 9.4% lower for design 2. The reason for this difference is due to the second segment climb gradient (SSCG) constraint, which requires the aircraft to have enough excess power to climb at a specified gradient with one engine out. Obviously, this requirement is more critical for the four engine design. Although design 2 need less thrust the propulsion system weight is 7.3% higher than design 1.

Cases 2 and 3: Case 2 has eight pylon mounted engines and case 3 has eight Boundary Layer Ingestion (BLI) inlet engines. This difference is modelled by eliminating the pylons and considering only half the wetted area of the nacelles for calculation of nacelle profile drag. We are assuming that the same sfc can be achieved with BLI inlets engines as pylon mounted engines. By eliminating the pylons the propulsion system weight decreases by 5.6% and the load alleviation is reduced. This gives an incentive to reduce the span and aspect ratio to reduce wing weight. The optimizer is able to this and still increase the lift-to-drag ratio by 2.8% since the nacelle drag has been reduced. As a result the fuel weight is reduced by 4.2% and $TOGW$ by

2.4%. The sfc has increased slightly (0.3%) since the thrust has been decreased by 1.7%.

Cases 3 and 4: At this point a part of the thrust is ducted out the trailing edge and the first effect of distributed propulsion is introduced, that is the effect on the induced drag. However, although the trailing edge is now used for longitudinal control the flaps are retained only for wing weight calculation. As can be seen from Table **??** the jet coefficient (C_J) is 0.032 and the resulting reduction in induced drag is only 0.5%. As a result the lift-to-drag ratio increases by approximately 0.1% and the fuel weight is reduced by 0.2%. This allows for a decrease span by 0.3 ft and a reduction in wing weight by 0.4% and $TOGW$ by 0.2%. It is clear from this that the induced drag effect is negligible.

Cases 4 and 5: By removing the trailing edge flaps the wing weight is reduced by 15,773 lb (12.1%). However, this weight reduction is also due to a 3.5 ft decrease in wing span. The lift-to-drag ratio is reduced by 1.5%, but the fuel weight is reduced by 1.3% since the $TOGW$ has been reduced by 21,174 lb (2.3%).

Cases 5 and 6: To simulate the duct weight the propulsion system weight is increased by 20%. Now the wing will have heavier engines and thereby the load alleviation is increased and the span and aspect ratio can be increased. In fact, the span increased by 3.1 ft and aspect ratio is increased from 4.25 to 4.32. However, in spite of this increase the lift-to-drag ratio decreases by 0.6%. The reason for this

reduction is not the reduced span efficiency (E) but the increase in trim drag. If the trim drag would be omitted from the calculation then the lift-to-drag ratio would be 24.71 for design 5 and 24.97 for design 6, which makes since design 6 has larger span and higher aspect ratio. The reason for the reduced span efficiency is caused by slightly different number of singularities used per section of wing in the induced drag module. The same span efficiency can be obtained for designs 5 and 6 by using the same number of singularities per section. This is a source of numerical noise and partly explains why convergence can be hard to achieve when small effects, like the induced drag effects, are introduced into the formulation. However, by adding the duct weight the $TOGW$ increases by 32,247 lb (3.7%) and the fuel weight increases by 13,317 lb (3.8%). Clearly, the duct weight has a significant effect on the weight and performance of the aircraft.

Cases 6 and 7: Here the duct efficiency is reduced from 100% to 95%. Since the ratio of profile drag and wave drag to total drag is approximately 0.506, the sfc has increased by 2.6%. This has led to an 3.2% increase in fuel weight, but the optimizer has also increased the span (by 1.2 ft) and aspect ratio (from 4.32 to 4.36) to increase the lift-to-drag ratio (by 0.5%) to reduce the effect of increased sfc. The $TOGW$ is increased by 1.7% or about 15,000 lb.

Cases 7 and 8: In this step the savings due to 'filling in' the wake is introduced. The objective was to find the savings that will give a distributed propulsion BWB design with approximately the same $TOGW$ as the conventional propulsion BWB in case

1. To achieve this, the distributed propulsion factor (η_{DP}) was varied from 0 - 100% in a step of 25% and optimum BWB designs were obtained for each step. The change in $TOGW$ with change in savings for each optimized design is shown in Figure 16. This graph shows that 100% of possible savings due to 'filling in' the wake is required to obtain a distributed propulsion BWB design, with η_d = 95% and w_d = 20%, that has approximately the same $TOGW$ as a conventional propulsion BWB. A comparison of the two optimized planforms is given in Figure 17. It is interesting to note how similar the planforms are. Both designs have wing span of approximately 239 ft and an aspect ratio of 4.28. Although their $TOGW$ are close, the weight distribution is different. The conventional propulsion BWB has a about 15,000 lb heavier wing, which is mostly due to trailing edge flap weight, than the distributed propulsion BWB. However, the propulsion system weight of the distributed propulsion BWB is approximately 10,000 lb heavier than its comparator. Furthermore, the distributed propulsion BWB has a 1.6% higher lift-to-drag ratio, but the cruise sfc is 3.8% higher due to smaller engines, yielding a 1.2% more fuel weight than the conventional propulsion BWB.

This MDO study of the effects of distributed propulsion shows that all of the possible savings due to 'filling in' the wake are required to obtain a 'conservative' distributed propulsion BWB design with a comparable $TOGW$ as a conventional propulsion BWB with four pylon mounted engines. As a further comparator, an 'optimistic' distributed propulsion BWB design was obtained. Figure 17 shows that about 65% of the possible

savings due to 'filling in' the wake are required to obtain a design with the same $TOGW$ as the conventional propulsion BWB. Schetz et al. [33] performed numerical simulations of jet-wing distributed propulsion flow fields of supercritical airfoil sections. The studies show that jet-wing distributed propulsion can be used to obtain propulsive efficiencies on the order of turbofan engine aircraft. If the trailing edge of the airfoil thickness is expanded, then jet-wing distributed propulsion can give up to an 8% improvement in propulsive efficiency. However, expanding the trailing edge must be done with care, as there is a drag penalty associated with it. It therefore seems unreasonable to design a distributed propulsion BWB with the same or comparable $TOGW$ as a conventional propulsion BWB. Significant weight penalty is associated with the distributed propulsion system that realistically cannot be overcome by the potential savings by effects on the induced drag, elimination of trailing edge flaps, and by 'filling in' the wake. However, other potential benefits of distributed propulsion that need to be considered when evaluating the overall performance of the design are

- Reduced total propulsion system noise,
- Improved safety due to engine redundancy,
- An engine-out condition is not as critical to the aircraft's performance in terms of loss of available thrust and controllability,
- The load redistribution provided by the engines has the potential to alleviate gust load/flutter problems, while providing passive load alleviation resulting in a lower

wing weight,

- Possible improvement in affordability due to the use of smaller, easily-interchangeable engines.

7 Conclusions

A model for distributed propulsion has been developed and implemented into an multidisciplinary design optimization (MDO) formulation for aircraft. The distributed propulsion concept considered here calls for a moderate number of engines distributed along the span of the wing of the aircraft. Part of the exhaust is ducted through the trailing edge of the wing, while the rest is exhausted through a conventional nozzle. A vectored thrust system applied to the trailing edge jet replaces evelons for longitudinal control and flaps.

The models developed include aerodynamics and propulsion interactions and the longitudinal vectored thrust control system. One of the important models developed is the effect of the trailing edge jet on the propulsive efficiency. An increase in propulsive efficiency can be attained when the engine jet is exhausted out the trailing edge of the wing, 'filling in' the wake that is created, and allowing for a better overall aerodynamic/propulsion system. The model considers the maximum and minimum attainable increase in propulsive efficiency for this system, and applies a part of that limit to the MDO formulation.

In addition to its effect on propulsive efficiency, the effect of the trailing edge jet on

the induced drag is modeled. This model adopts the formulation suggested by Spence [14, 15, 16], where the induced drag is reduced through the jet coefficient C_J. Other models include the controls/propulsion integration, thrust losses due to the ducting, and the increase in propulsion weight due to the weight of the duct.

The Blended Wing Body (BWB) aircraft was used as a testbed to study the distributed propulsion concept. The distributed propulsion models were integrated into a BWB MDO formulation. The MDO framework was validated by analyzing published Boeing BWB designs.

Two different BWB configurations were optimized. A conventional propulsion BWB with four pylon mounted engines and two versions of a distributed propulsion BWB with eight boundary layer ingestion inlet engines. A 'conservative' distributed propulsion BWB design with 20% duct weight factor and a 95% duct efficiency, and an 'optimistic' distributed propulsion BWB design with 10% duct weight factor and a 97% duct efficiency. The results show that a 65% of possible savings due to 'filling in' the wake are required for the 'optimistic' distributed propulsion BWB design to have comparable $TOGW$ as the conventional propulsion BWB, and 100% savings are required for the 'conservative' design. Therefore it is not realistic to achieve such a design. Significant weight penalty is associated with the distributed propulsion system that realistically cannot be overcome by the potential savings by effects on the induced drag, elimination of trailing edge flaps, and by 'filling in' the wake.

Intermediate optimum designs reveal that the savings in $TOGW$ are due to elimination

of the trailing edge flaps and the increase in propulsive efficiency due to 'filling in' the wake. The savings due to the effect of the jet on the induced drag is negligible. The adverse effects of having a distributed propulsion system are the added duct weight and thrust loss due to the ducting some of the exhaust out the trailing edge. Furthermore, distributed propulsion requires a moderate amount of small engines distributed along the span of the wing. Smaller engines are not as efficient as larger ones, since they have higher specific fuel consumption. This is one of the biggest reasons why distributed propulsion has significant weight penalty.

Clearly, there is a need to obtain a physics-based model of the duct weight and duct efficiency. The most obvious way is to represented the duct by two flat plates, positioned closely to each other, with the exhaust flowing between them. With this arrangement the duct weight can be easily estimated. Furthermore, duct efficiency could be estimated by analyzing the flow between the two plates. This arrangement has the potential of giving a realistic representation of the performance and weight of the ducts, but needs to be investigated further before implementing in the MDO framework.

Although significant weight penalty is associated with the distributed propulsion system presented in this study other characteristics need to be considered when evaluating the overall effects. Potential benefits of distributed propulsion are for example reduced propulsion system noise, improved safety due to engine redundancy, less critical engine-out condition, gust load/flutter alleviation, increased affordability due to smaller, easily-interchangeable engines.

8 Acknowledgements

This work was partly supported by the Systems Analysis Branch at NASA Langley. We would like to acknowledge their help with information, insight and material. We would like to specifically acknowledge William M. Kimmel and Mark Guynn at NASA Langley for their support and help in this work. Also, we would like to thank Dino Roman at Boeing for his assistance and comments on the BWB weight analysis.

References

[1] Ashley, H. "On Making Things the Best-Aeronautical Uses of Optimization". *Journal of Aircraft*, **19**(1):5–28, January 1982.

[2] Sobieszczanski-Sobieski, J. and Haftka, R. T. "Multidisciplinary Aerospace Design Optimization: Survey of Recent Developments". *Structural Optimization*, **14**(1):1–23, 1997.

[3] Kroo, I. "MDO Applications in Preliminary Design: Status and Directions". *AIAA 97-1408*, 1997.

[4] Liebeck, R. "Design of the Blended-Wing-Body Subsonic Transport". *AIAA Aerospace Sciences Meeting and Exhibit, AIAA-2002-0002, Reno, NV*, January 14-17 2002.

[5] NASA Aeronautics Blueprint: Toward a Bold New Era in Aviation.

[6] Solies, U. P. "Flight Measurements of Downwash on the Ball-Bartoe Jetwing Powered Lift Aircraft". *Journal of Aircraft*, **29**(5):927–931, Sept.-Oct. 1992.

[7] Harris, K. D. "The Hunting H.126 Jet Flap Aircraft". *AGARD Assessment of Lift Augmentation Devices, Lecture Series 43*, Feb. 1971.

[8] Attinello, J. S. "The Jet Wing". *IAS Preprint No. 703, IAS 25th Annual Meeting*, pages 10–11, Jan. 28-31 1957.

[9] Marine Engineering, Vol. 1. *Society of Naval Architect and Marine Engineers, Ed. Herbert Lee Seward*, pages 10–11.

[10] Ko, A. "The Multidisciplinary Design Optimization of a Distributed Propulsion Blended-Wing-Body Aircraft". *Ph.D. Dissertation, Virginia Polytechnic Institute and State University*, April 2003.

[11] Ko, A., Schetz, J. A., and Mason, W. H. "Assessment of the Potential Advantages of Distributed Propulsion for Aircraft". *16th International Symposium on Air Breathing Engines (ISABE), ISABE-2003-1094, Cleveland, OH*, Aug. 31-Sept. 5 2003.

[12] Hill, P. and Peterson, C. *Mechanics and Thermodynamics of Propulsion, 2nd Edition.* Addison-Wesley, New York, 1992.

[13] Stinton, D. *The Anatomy of the Airplane, 2nd Edition.* American Institute of Aeronautics and Astronautics, Reston, VA, 1998.

[14] Spence, D. A. "The Lift Coefficient of a Thin, Jet-Flapped Wing". *Proceedings of the Royal Society of London*, **238**(121):46–68, Dec. 1956.

[15] Spence, D. A. "A Theory of the Jet Flap in Three Dimensions". *Proceedings of the Royal Society of London*, **251**(1266):407–425, June 1959.

[16] Spence, D. A. "The Lift Coefficient of a Thin, Jet-Flapped Wing. II. A Solution of the Integro-Differential Equation for the Slope of the Jet". *Proceedings of the Royal Society of London*, **261**(1304):97–118, Apr. 1961.

[17] Liebeck, R., Page, M.A., Rawdon, B.K., Scott, P.W., and Wright, R.A. "Concepts for Advanced Subsonic Transports". *NASA CR 4624*, Sept. 1994.

[18] Grasmeyer, J.M., Naghshineh, A., Tetrault, P.A., Grossman, B., Haftka, R.T., Kapania, R.K., Mason, W.H., and Schetz, J.A. "Multidisciplinary Design Optimization of a Strut-Braced Wing Aircraft with Tip-Mounted Engines". *MAD Center Report MAD-98-01-01*, January 1998.

[19] Grasmeyer, J.M. "A Discrete Vortex Method for Calculationg the Minimum Induced Drag and Optimum Load Distribution for Aircraft Configurations with Noncoplanar Surfaces". January 1998.

[20] Malone, B. and Mason, W.H. "Multidisciplinary Optimization in Aircraft Design Using Analytic Technology Models". *Journal of Aircraft*, **32**(2):431–438, March–April 1995.

[21] Braslow, A.L., Maddalon, D.V., Bartlett, D.W., Wagner, R.D., and Collier, F.S. "Applied Aspects of Laminar-Flow Technology". *Viscous Drag Reduction in Boundary Layers*, pages 47–78, 1990.

[22] Boltz, F.W., Renyon, G.C., and Allen, C.Q. "Effects of Sweep Angle on the Boundary Layer Stability Characteristics of an Untapered Wing at Low Speeds". *NASA TN D-338*, 1960.

[23] Lamar, J.E. "A Vortex Lattice Method for the Mean Camber Shapes of Trimmed Non-Coplanar Planforms with Minimum Vortex Drag". June 1976.

[24] Gundlach, J.F. "Multidisciplinary Design Optimization and Industry Review of a 2010 Strut-Braced WIng Transonic Transport". *M.Sc. Thesis, Virginia Polytechnic Institute and State University*, June 1999.

[25] Gorton, S.A., Owens, L.R., Jenkins, L.N., Allan, B.G., and Schuster, E.P. "Active Flow Control on a Boundary-Layer-Ingesting Inlet", AIAA Paper 2004-1203, 2004 .

[26] Gern, F.H., Gundlach, J.F., Naghshineh-Pour, A., Sulaeman, E., Tetrault, P.A., Grossman, B., Kapania, R.K., Mason, W.H., Schetz, J.A., and Haftka, R.T. "Multidisciplinary Design Optimization of a Transonic Commercial Transport with a Strut-Braced Wing", World Aviation Conference and Exposition, SAE 1999-01-5621, San Francisco, CA, Oct., 1999 .

[27] McCullers, L.A. FLOPS User's Guide, Release 5.81.

[28] Torenbeek, E. Synthesis of Subsonic Airplane Design. 1982.

[29] Roskam, J. and Lan, C.T.E. Airplane Aerodynamics and Performance. 1997.

[30] Laban, M., Arendsen, P., Rouwhorst, W., and Vankan, W. "A Computational Design Engine for Multi-Disciplinary Optimization with Application to a Blended Wing Body Configuration". Sept. 4–6 2002.

[31] Liebeck, R.H. "Design of the Blended Wing Body Subsonic Transport". *Journal of Aircraft*, **41**(1):10–25, January–February 2004.

[32] Roman, D., Allen, J.B., and Liebeck, R.H. "Aerodynamic Design Challenges of the Blended-Wing-Body Subsonic Transport", AIAA Paper 2000-4335, 2000 .

[33] Schetz, J.A., Hosder, S., Walker, J., and Dippold, V. "Numerical Simulation of Jet-Wing Distributed Propulsion Flow Fields", ISABE-2005-1123, Sept., 2005 .

Table 1: Design Variables

Nr.	Design Variable	Description	Range
1	b	Wing span	120.0 - 264.2 ft
2	η_2	Span station #2	0.05 - 0.50
3	Δ_1	Span increment ($\eta_3 = \eta_2 + \Delta_1$)	0.10 - 0.50
4	Δ_2	Span increment ($\eta_4 = \eta_3 + \Delta_2$)	0.10 - 0.25
5-9	c_i	Chord at span station i ($i = 1, ..., 5$)	10 - 300 ft
10-14	t_i	Thickness at span station i ($i = 1, ..., 5$)	0.5 - 30 ft
15-18	Λ_i	Quarter chord sweep at section i ($i = 1, ..., 4$)	0 - 60 deg.
19	x_{LE}	Leading edge clearance in front of cabin	0 - 30 ft
20	x_{Cabin}	Cabin length at center of aircraft	50 - 150 ft
21	W_{fuel}	Fuel weight	148,000 - 592,000 lb
22	T_{sls}	Sea level static thrust per engine	5,560 - 111,200 lb
23	h_{cruise}	Average cruise altitude	17.5 - 50.0 kft

Table 2: Design Constraints

Nr.	Constraint	Description
1	Range	$\geq$ 7,750 nm
2	Fuel Capacity	Fuel Volume $\leq$ Fuel Tank Volume
3	Balanced Field Length	$\leq$ 11,000 ft
4	Second Segment Climb Gradient	$\geq 2.7^o$
5	Missed Approach Climb Gradient	$\geq 2.4^o$
6	Rate of Climb at Top of Climb	$\geq$ 300 ft/min
7	Landing Distance	$\leq$ 11,000 ft
8	Approach Velocity	$\leq$ 140 knots
9-13	Longitudinal Stability and Control	See section 4.7
14	Cabin Area	$\geq$ 4,000 sqft
15-24	Wing Thickness	See section 4.2
25	Span station limitation	$\eta_4 \leq 0.8$
26	TE sweep at section 1	$\Lambda_{TE_1} \geq 0$
27	TE sweep at section 3	$\Lambda_{TE_3} \leq 0$

Table 3: Design Parameters

Nr.	Parameter	Description	Value
1	M	Cruise Mach number	0.85
2	R	Range	7,750 nm
3	R_{res}	Reserve range	500 nm
4	N_{pax}	Number of passengers	478
5	N_{eng}	Number of engines	4-8
6	η_{DP}	Distributed propulsion factor	0 - 100%
7	η_d	Duct efficiency	95-97%
8	w_d	Duct weight factor	10-20%

Table 4: Weight analysis of a BWB-450-like aircraft with a mission of 478 passengers and 8,700 nm range at cruise Mach 0.85.

Component	Weight (lb)
Wing	131,375
Cabin and afterbody *	85,572
Landing gear	50,740
Propulsion system (3 engines)	62,774
Subsystems †	123,125
Operational Empty Weight	453,586
Payload (480 pax)	105,160
Zero Fuel Weight	558,756
Fuel Weight	390,720
TOGW	949,466

*Includes a weight penalty of 15,000 lb due to the unconventionality of the cabin pressure vessel.

†Includes a weight penalty of 10%. Added after interaction with Boeing staff.

Table 5: An outline of a MDO study of intermediate distributed propulsion effects. Table key: CP = Conventional Propulsion, DP = Distributed Propulsion, PM = Pylon Mounted, BLI = Boundary Layer Ingesting Inlet.

Nr.	Propulsion Configuration	Number of Engines	Engine Configuration	DP Effects	Other Properties
1	CP	4	PM	N/A	-
2	CP	8	PM	N/A	-
3	CP	8	BLI	N/A	No Pylons and $1/2 S_{wet_{nac}}$
4	DP	8	BLI	Induced drag	With flaps
5	DP	8	BLI	Induced drag	Without flaps
6	DP	8	BLI	Duct weight	$w_d = 10 - 20\%$
7	DP	8	BLI	Duct efficiency	$\eta_d = 95 - 97\%$
8	DP	8	BLI	DP factor	$\eta_{DP} = 0 - 100\%$

Table 6: Optimum configuration comparisons between the conventional propulsion and distributed propulsion BWB designs, along with intermediate optimum designs showing the individual distributed propulsion effects.

Case Number	**1**	**2**	**3**	**4**	**5**	**6**	**7**	**8**
Propulsion Configuration	CP	CP	CP	DP	DP	DP	DP	DP
Engine Configuration	PM	PM	BLI	BLI	BLI	BLI	BLI	BLI
Distributed Propulsion Effects				Induced Drag	Induced Drag	Duct Weight	Duct Efficiency	Propulsive Efficiency
Other Properties		N/A	No Pylons 1/2 Nacelle	Flaps On	Flaps Off			
Parameters								
Number of Engines	4	8	8	8	8	8	8	8
Duct Weight Factor				1.00	1.00	1.20	1.20	1.20
Duct Efficiency		N/A		1.00	1.00	1.00	0.95	0.95
Distributed Propulsion Factor				0.00	0.00	0.00	0.00	1.00
Design Variables								
Wing Span (ft)	239.5	245.5	242.7	242.4	238.9	242.0	243.2	239.3
Average Cruise Altitude (ft)	36,475	36,048	35,799	35,802	36,113	35,979	35,964	35,341
Max SLS Thrust per engine (lb)	56,708	25,698	25,265	25,126	24,924	25,671	25,984	24,296
Max SLS Total Thrust (lb)	226,832	205,587	202,117	201,011	199,392	205,364	207,872	194,365
Fuel Weight (lb)	314,330	365,983	351,510	349,714	346,009	358,425	369,908	318,374
Fuel Weight + Correction (lb)	315,224	367,102	351,666	350,848	346,272	359,589	370,197	318,939
Aircraft Properties								
TOGW (lb)	860,936	926,871	904,691	901,884	880,710	912,056	927,222	860,769
TOGW + Correction (lb)	861,830	927,990	904,848	903,018	880,973	913,220	927,510	861,334
Wing Weight (lb)	127,934	133,863	131,062	130,486	114,713	117,886	119,984	113,200
Propulsion System Weight (lb)	59,414	63,767	60,211	59,925	59,505	73,258	74,029	69,829
Wing Area (sqft)	13,400	13,538	13,436	13,430	13,440	13,542	13,566	13,378
Aspect Ratio	4.28	4.45	4.38	4.38	4.25	4.32	4.36	4.28
L/D @ Cruise	23.90	24.23	24.90	24.92	24.54	24.39	24.52	24.28
C_L @ Cruise	0.223	0.229	0.223	0.223	0.220	0.225	0.227	0.211
E	0.944	0.934	0.937	0.937	0.944	0.936	0.935	0.938
sfc @ Cruise (lb/hr/lb)	0.579	0.657	0.659	0.659	0.659	0.657	0.674	0.601
DP Properties								
C_J	0	0	0	0.032	0.033	0.032	0.031	0.031
C_{DiDP}/C_{Di}	1	1	1	0.995	0.995	0.995	0.995	0.995
Θ	0.502	0.496	0.520	0.522	0.525	0.509	0.506	0.537
T_{net}/T	1	1	1	1	1	1	0.974	0.973

Figure 1: A blended-wing-body aircraft with a conventional propulsion arrangement. Picture by the Boeing company.

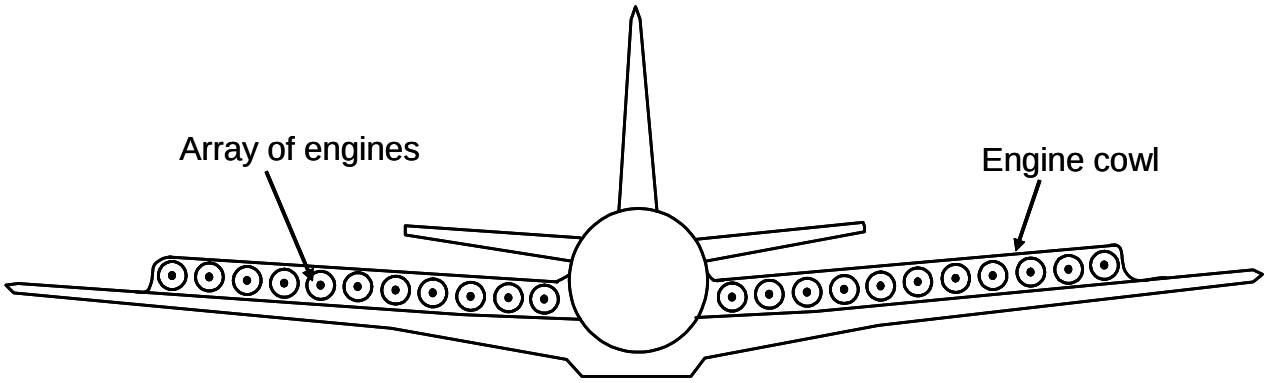

Figure 2: Front view schematic of a distributed propulsion configuration with an array of small engines distributed along the wing. This arrangement has been determined unattractive.

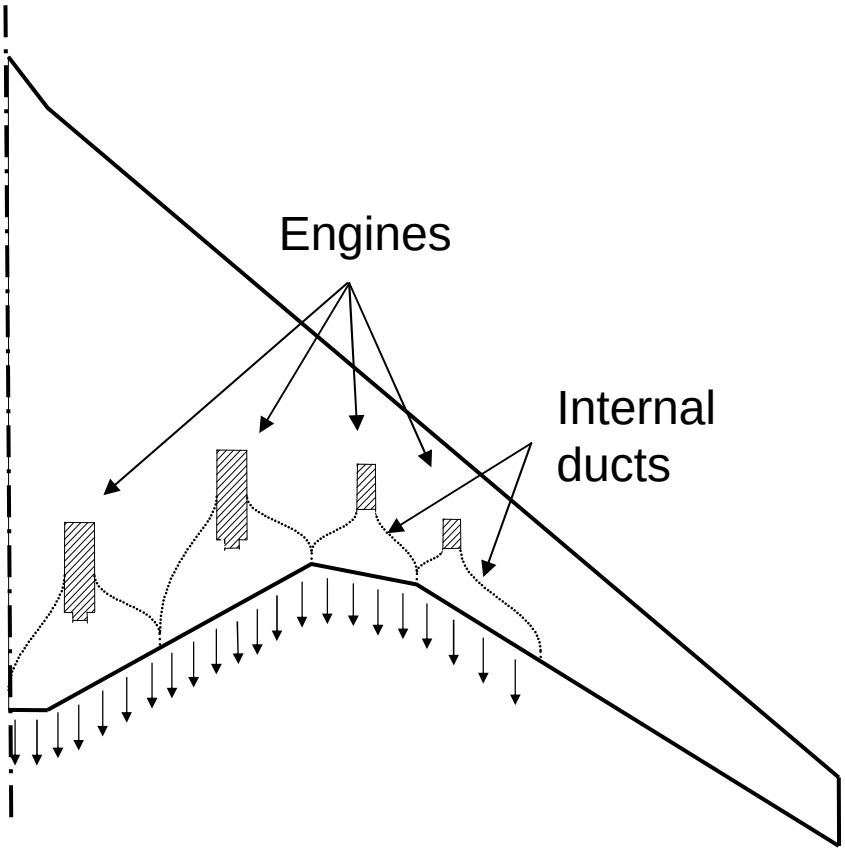

Figure 3: A planform view of a BWB with distributed propulsion configuration as proposed in this work.

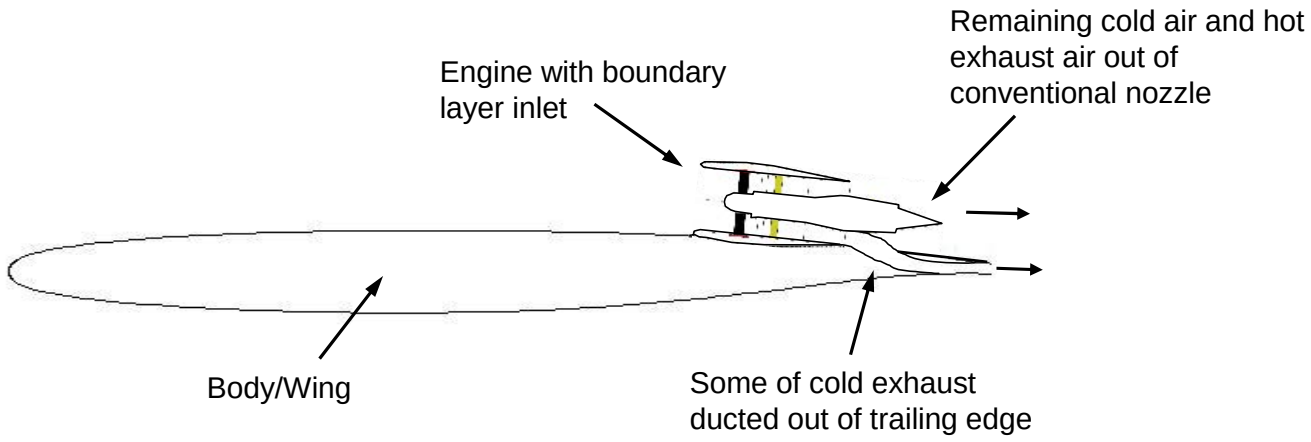

a) Streamwise cut through a section with an engine

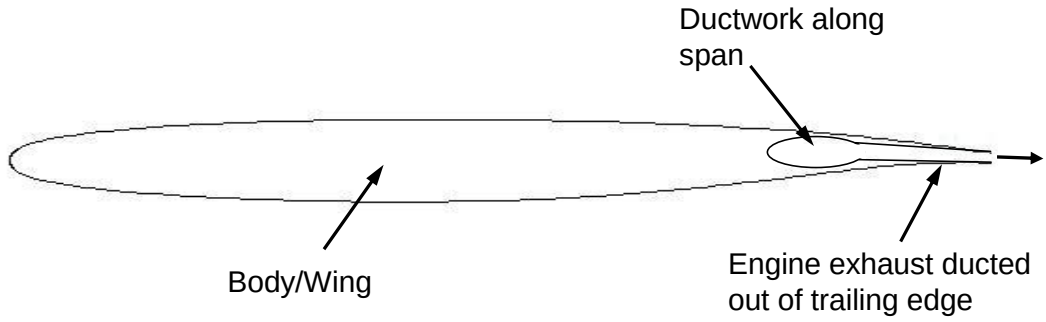

b) Streamwise cut through a section between engines

Figure 4: Wing streamwise cross-sections at a location with an engine and at a location between engines.

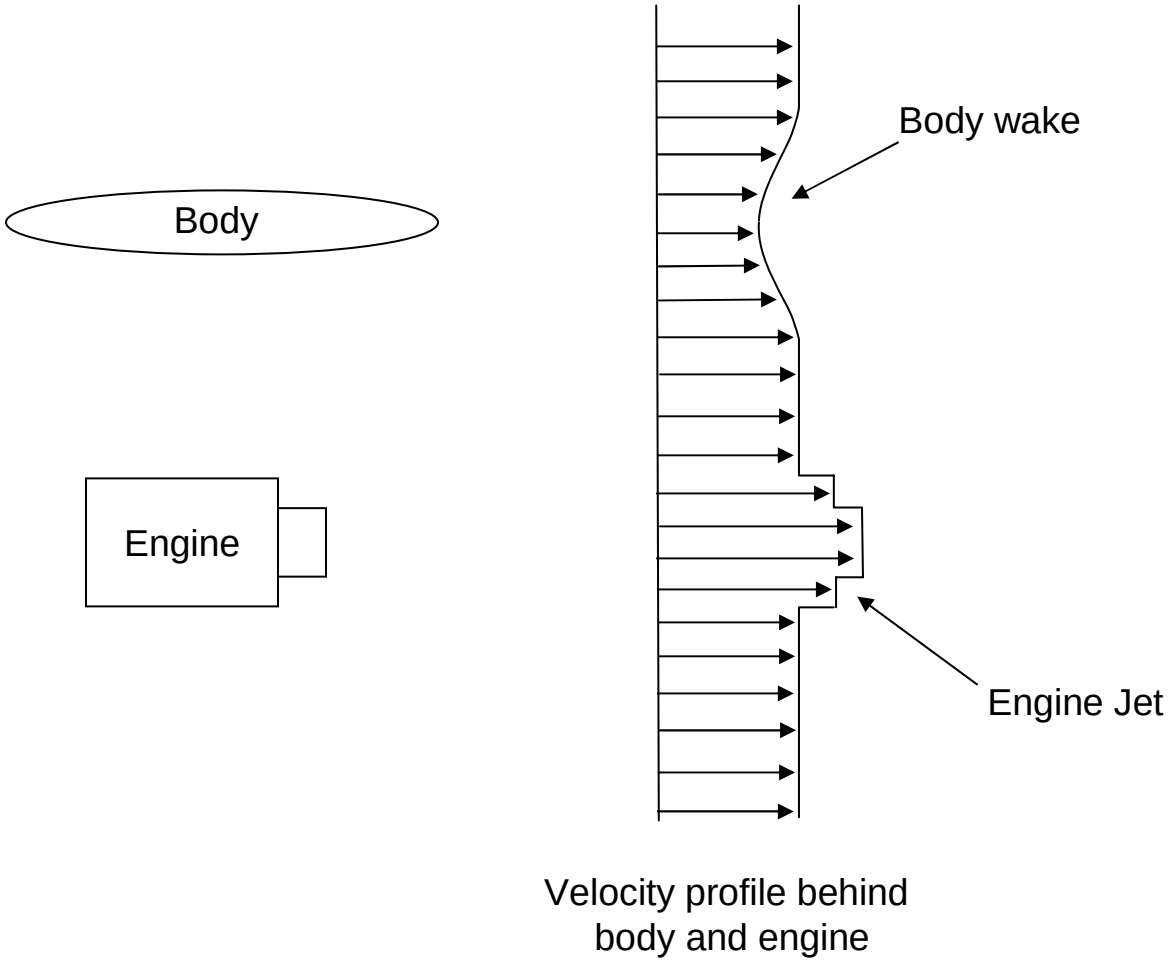

Figure 5: A typical velocity profile behind a body and an engine.

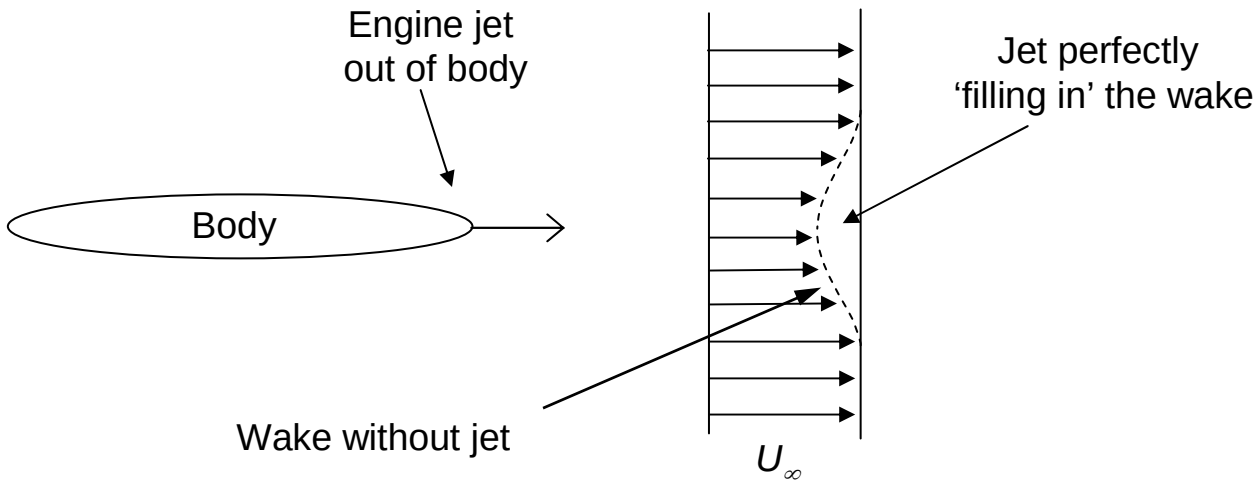

Figure 6: A velocity profile of an ideal distributed propulsion body/engine system.

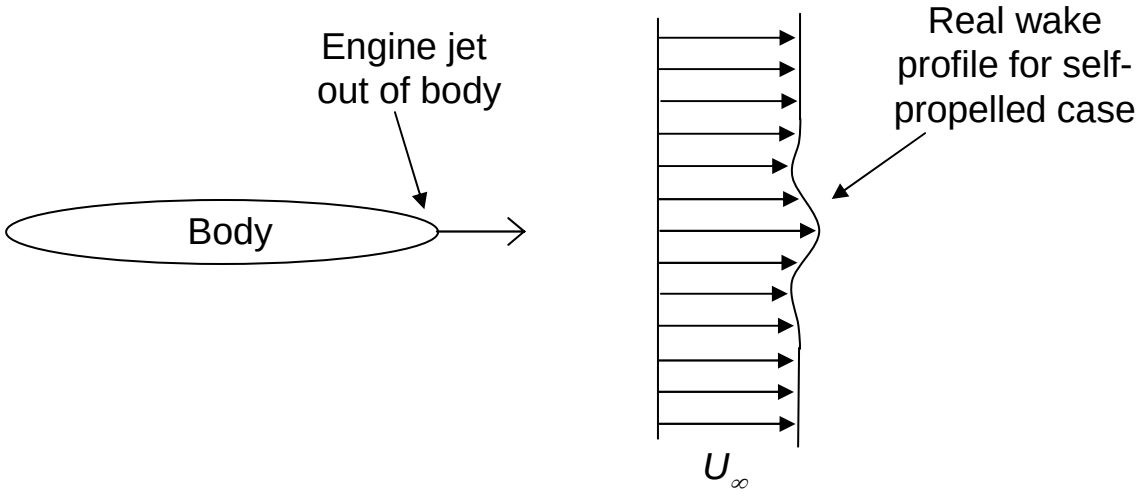

Figure 7: A velocity profile of a realistic distributed propulsion body/engine system.

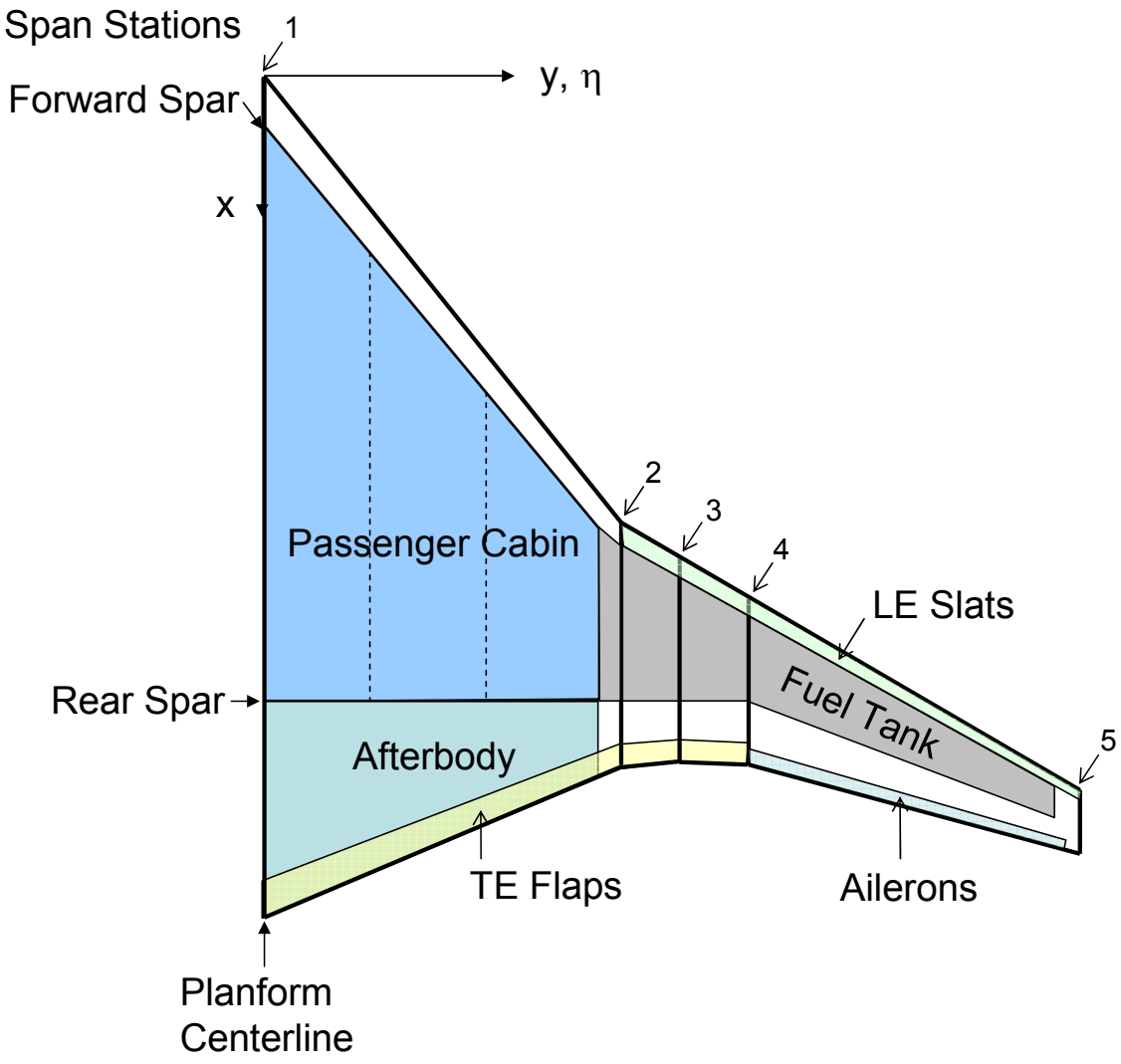

Figure 8: The BWB planform showing the five span stations, locations of the passenger cabin, afterbody, fuel tanks, and high lift systems.

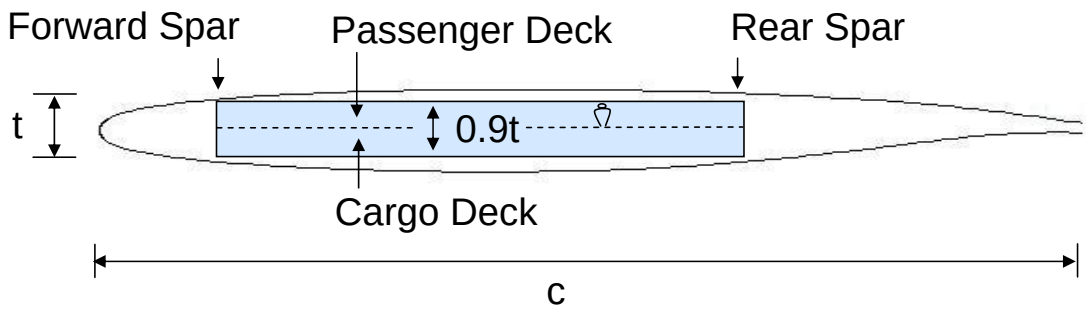

Figure 9: A cross section of the BWB showing the double decked center section containing the passenger and cargo decks.

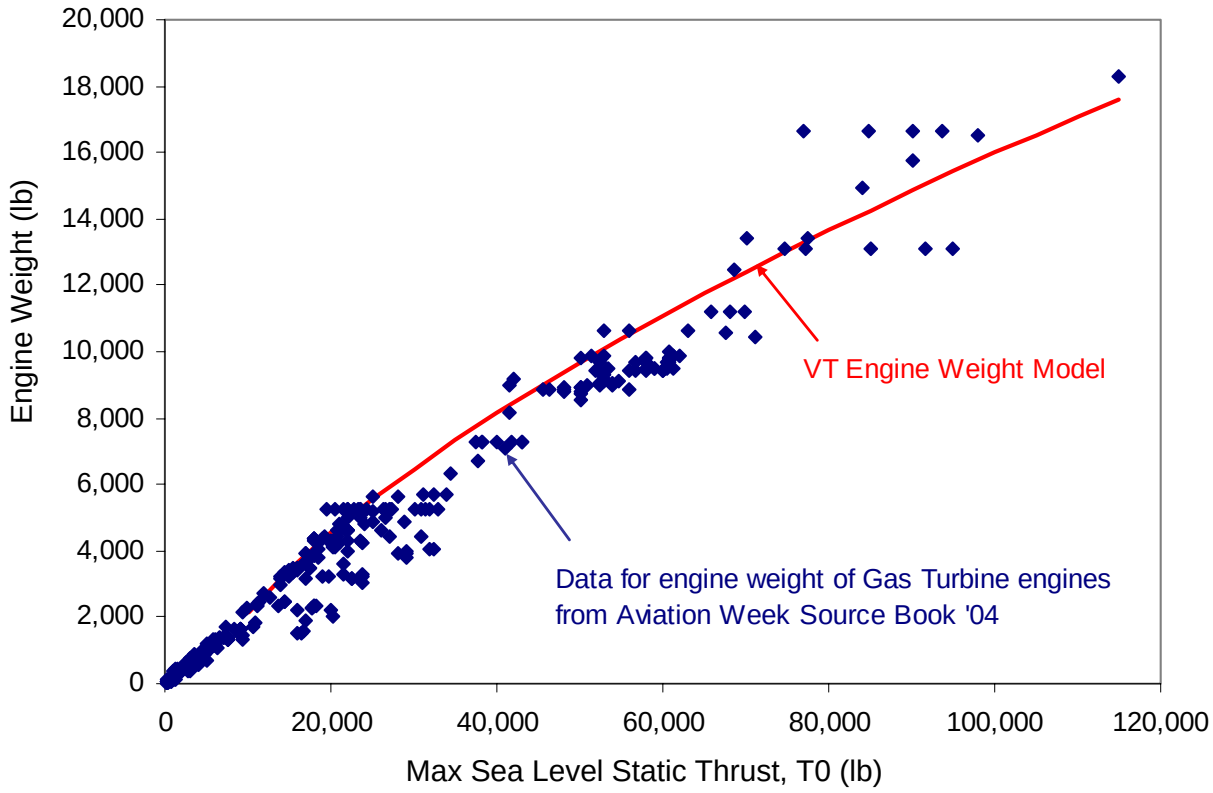

Figure 10: Comparison of Virginia Tech's (VT) engine weight model with engine weight data for turbofan and turbojet engines.

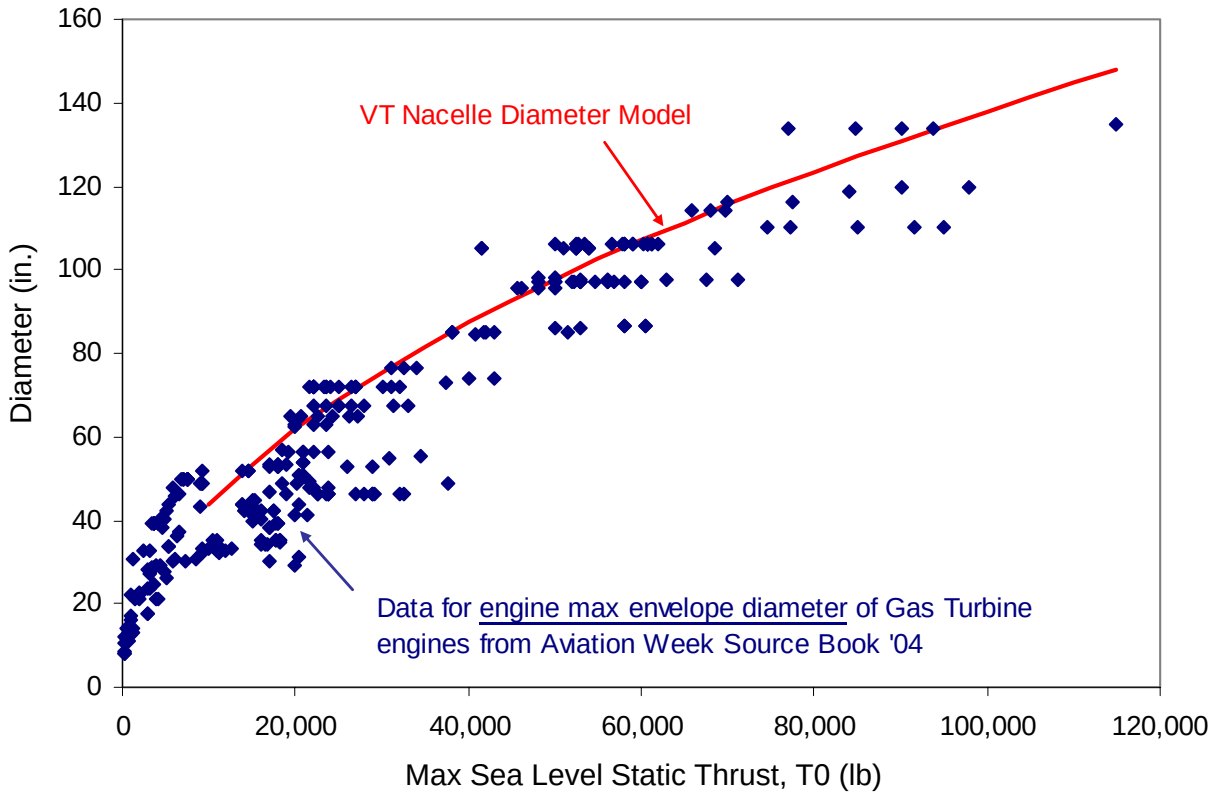

Figure 11: Comparison of VT's nacelle diameter model with engine maximum envelope diameter of turbofan and turbojet engines.

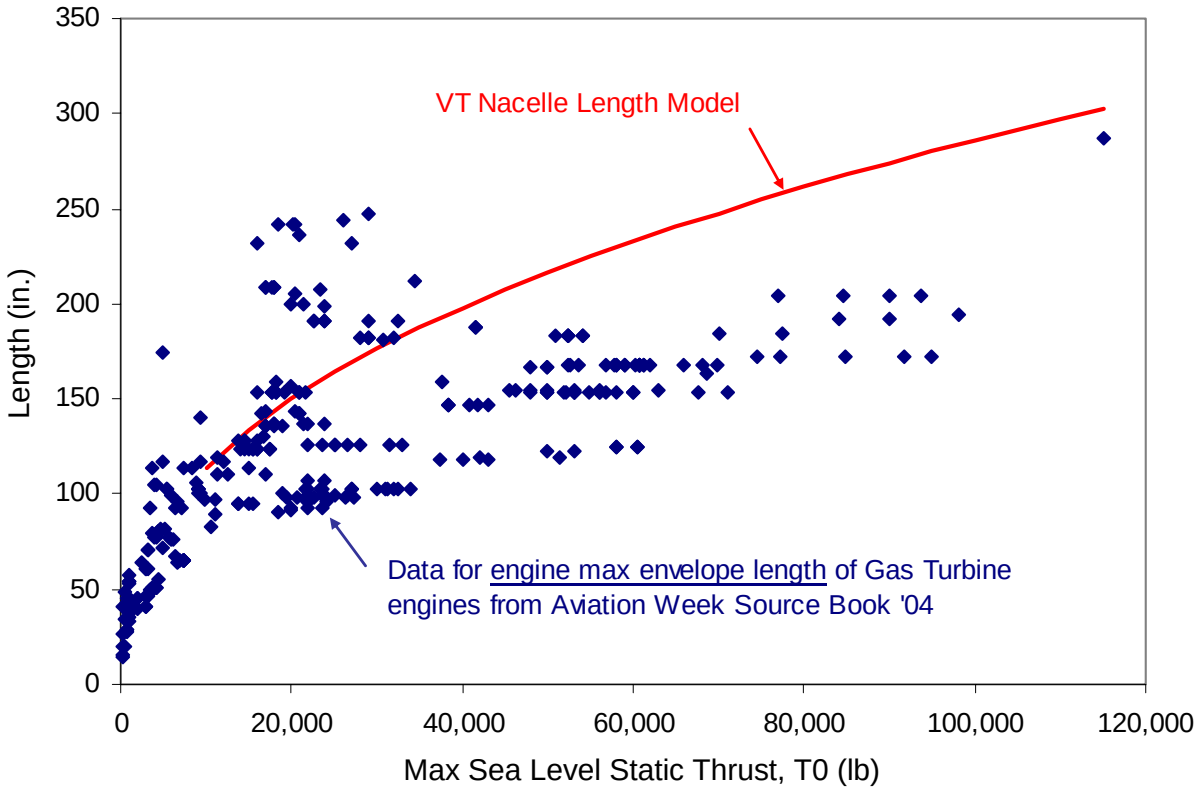

Figure 12: Comparison of VT's nacelle length model with engine maximum envelope length of turbofan and turbojet engines.

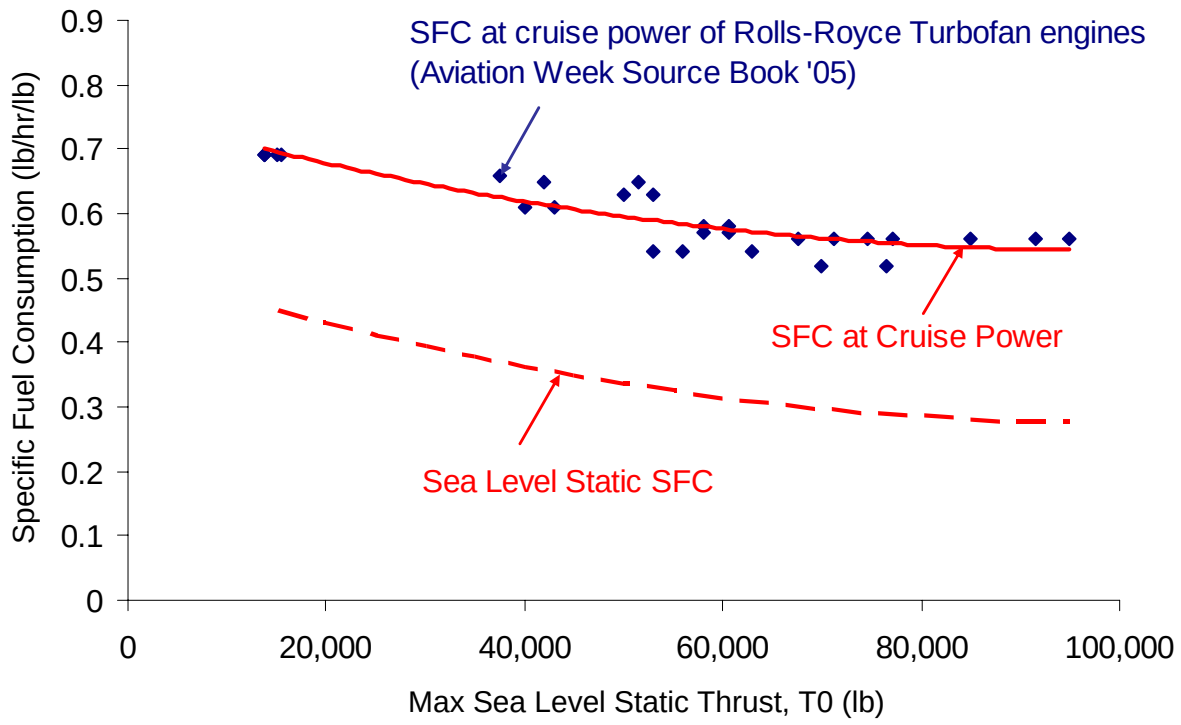

Figure 13: Second order polynomial correlation of specific fuel consumption (sfc) at cruise power with maximum sea level static thrust for data of Rolls-Royce engines. Based on the cruise power (assuming an altitude of 30 kft and Mach 0.85) sfc correlation and Gundlach's sfc model (Eq. 17), the curve for the sea level static sfc is obtained.

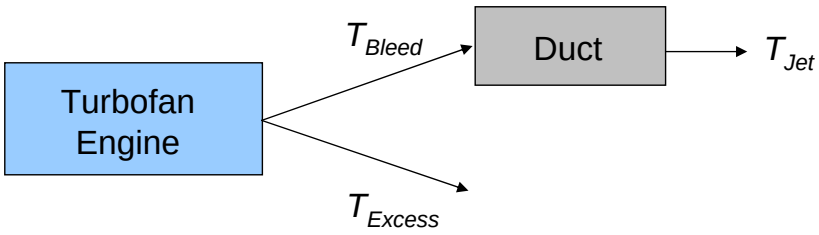

Figure 14: A schematic showing how the bleed part of the turbofan engine exhaust is diverted through a duct and the excess part out the rear.

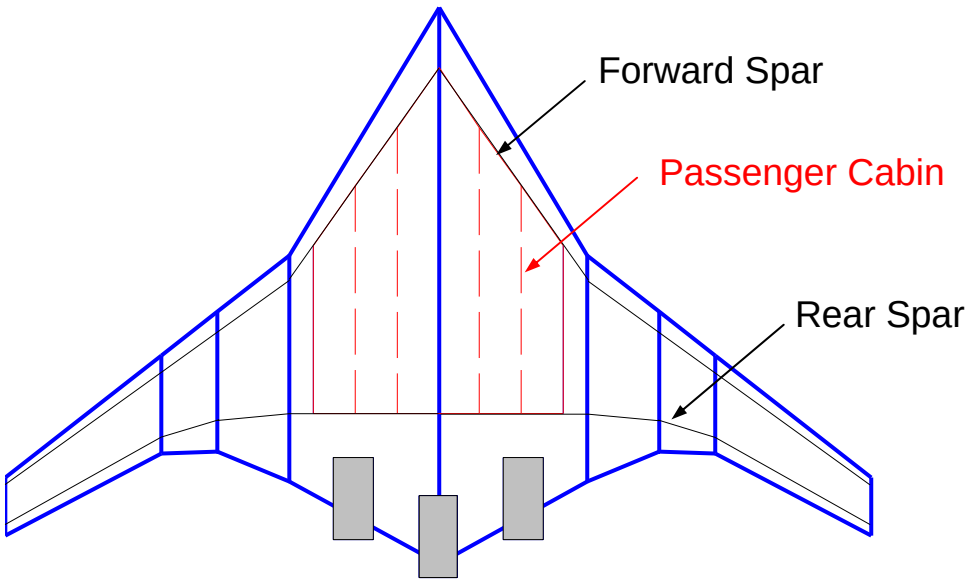

TOGW = 949,466 lb
L/D @ Cruise = 21.7
C_L *@ Cruise* = 0.216
E = 1.01
sfc @ Cruise = 0.544 lb/hr/lb

Figure 15: Analysis of a BWB-450-like aircraft with a mission of 478 passengers and 8,700 nm range at cruise Mach 0.85.

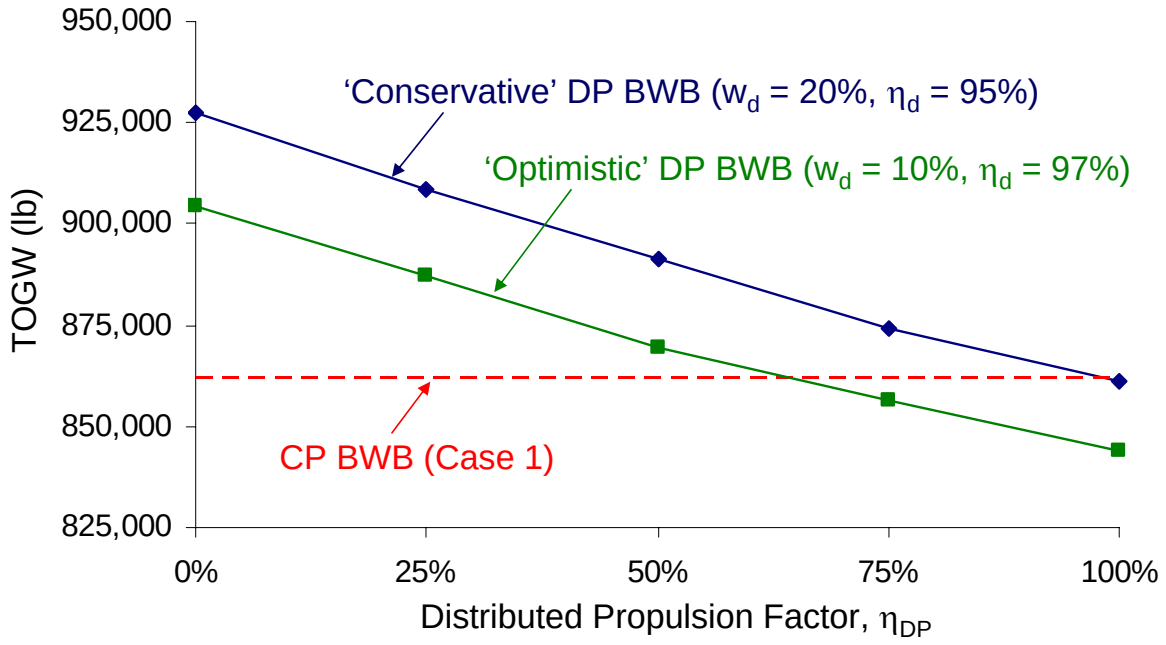

Figure 16: The change in $TOGW$ of a distributed propulsion (DP) BWB with change in possible savings by 'filling in' the wake for the cases of an 'optimistic' ($w_d = 10\%$, $\eta_d = 97\%$) design and a 'conservative' ($w_d = 20\%$, $\eta_d = 95\%$) design, compared with the $TOGW$ of a conventional propulsion (CP) BWB (4 engines).

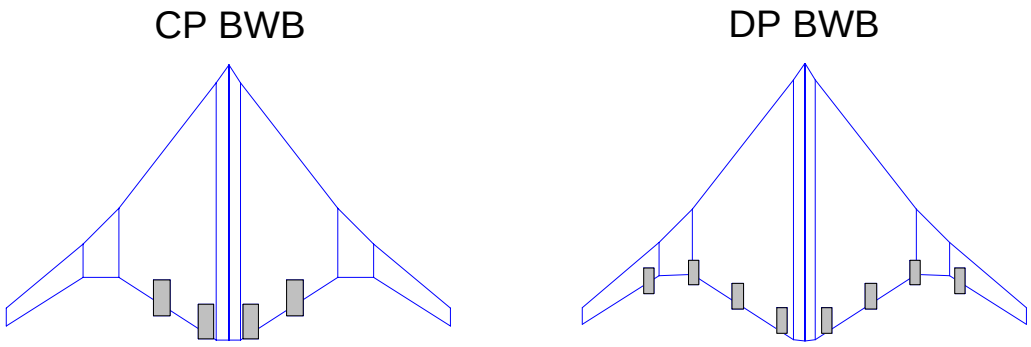

TOGW (lb)	860,936	860,769
L/D @ Cruise	23.90	24.28
CL @ Cruise	0.223	0.211
sfc @ Cruise (lb/hr/lb)	0.579	0.601

Figure 17: Comparison of the optimum configuration design of the conventional propulsion (CP) BWB (Case 1) and a distributed propulsion (DP) BWB (Case 8 with $w_d = 20\%$ and $\eta_d = 95\%$).